Improved waveguide structures derived from new rapid optimization techniques

T. P. Felici, D. F. G. Gallagher

Photon Design (United Kingdom)

ABSTRACT

We present structures obtained with numerical optimization techniques capable of efficiently channeling light at a fraction of the length of a conventional taper. These results could open the way to novel designs in ultra-short light injection devices. We also consider the rather different problem of how to optimise the transmission through a photonic crystal bend. We show how, using a deterministic global optimisation algorithm, novel optimal geometries can be obtained leading to considerable performance improvements.

Keywords: Waveguide modelling, taper injectors, photonic crystals, local optimisation, global optimisation.

OPTIMISING INJECTOR DEVICES

Tapered waveguides, where the cross-section varies monotonically and continuously along the propagation direction, are widely used in photonics to couple light between waveguides of different shapes. It is well known that the power lost through the taper side-walls decreases for increasing taper lengths, becoming effectively loss-less or "adiabatic" for large lengths [1-3]. This is due to the fact that if the cross sectional variation is slow enough over length-scales corresponding to the intermodal beatlengths, the cross coupling between guided modes becomes negligible. For practical reasons however, it is desirable to keep the taper length as short as possible.

In this study we describe a technique we successfully used to create novel designs of very short injection devices capable of efficiently transmitting light from large input devices to small output devices. We then discuss the results we obtained for an example problem, and the possible applications.

THE EXAMPLE PROBLEM

We consider a glass uniform waveguide (refractive index 1.51) interfacing to air, with a width of 7 μm. The output waveguide is of the same material, but with a width of 0.5 μm. We choose the working wavelength to be 1.51 μm. In this presentation we consider a two-dimensional model of this structure. The same design approach, however, will work for more general 3D structures.

The first stage in designing the injecting intermediate device is to decide its desired composition. The most obvious choice in this example is to choose a z-varying waveguide with the same refractive index in the core and cladding as the end waveguides. We also assume that due to design constraints, it is desirable to fix the injector length to 7 μm. We begin with choosing the trial initial shape to be a linear tapered profile. This means that the taper has an angle of 45 degrees. We therefore expect the losses to be very high. We note that for adiabaticity to be achieved we would require lengths greater than 40 μm, i.e. at least 6 times this length.

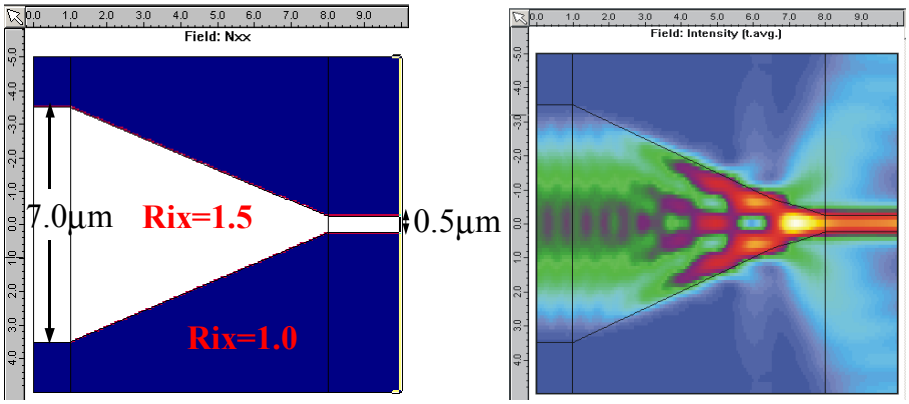

Fig. 1. Initial 2D model of an injector design. The linear taper model has an efficiency of merely 53%, most of the power being lost to radiation.

SOLVING THE PROPAGATION PROBLEM.

A necessary requirement is the availability of a robust field calculation engine capable of modeling such wide angle, high contrast structures. While classical Beam Propagation Methods (BPMs) can be used to determine propagation in low-index-contrast, small-angle tapers [4], clearly classical BPMs are inadequate here. Wide angle BPMs could be used, but even these have a limit in the profiles they can accurately compute. Instead the commercial propagation tool FIMMPROP by Photon Design was used [5], which solver propagation problems using the Mode Matching Method (MMM). This consists of subdividing the taper into thin, z-invariant sections. Sufficient local guided and radiation modes ψ_m, with corresponding propagation constants β_m, are computed in each of these sections to represent the EM field Φ with sufficient accuracy:

$$\Phi(x,y,z) = \sum_{m>=1} \psi_m(x,y) \cdot (c_m^+ . e^{i\beta_m z} + c_m^- . e^{-i\beta_m z})$$

The field in the entire device is then given by a scattering matrix approach involving both forward and backward modal excitations c_m^+, c_m^- for the field in each of these sections. This technique is known to rigorously solve the wave equations, on the condition of having sufficient local modes, implicitly accounting for internal reflections and propagation at any angle. Moreover, MMM naturally provides the data we require, as the transmission efficiency is none other that the modal excitation in the fundamental mode of the exit waveguide:

$$P = c_1^+$$

Using MMM we calculated the power transmission in our initial linear taper to be just over 50%, meaning that most of the power is lost to radiation (Fig. 1).

THE OPTIMIZATION PROBLEM

We now model the taper shape as a piecewise linear function (Fig. 2). The cross-sectional widths at the function nodes will be the parameters varied in the optimization process. The resulting transmission P therefore becomes a function of these parameters. We also impose the shape to remain laterally symmetric.

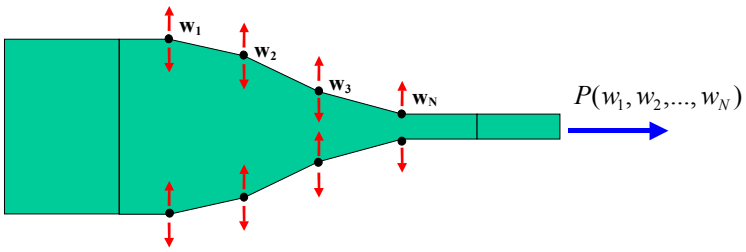

Fig. 2. Piece wise linear parameterization of the taper shape in terms of cross-sectional widths at the nodes. The resulting transmission P therefore becomes a function of these parameters.

The commercial optimisation package KALLISTOS [8] was used for performing the optimisations. This package is specialized for the optimisation of waveguide problems and comes with several optimisation techniques. The Quasi-Newton method provided therein was applied to find the values for these parameters giving the best power transmission. This is a local descent technique giving second order convergence near the optimal solution.

The derivatives of P with respect to each of its parameters are required. These could be calculated using finite differences, but that would require N field calculations per optimization step (one for each derivative). It is however possible to calculate these analytically by exploiting the linear structure of the wave equations. Indeed these techniques are incorporated in KALLISTOS, leading to an N fold speed improvement in the calculation of each descent step!

THE RESULTS: THE MODAL RESONANCE EFFECT.

Fig. 3 shows the shape we obtained after 20 iterations of the optimization process. This shape has a transmission of 90%! We used 9 nodes, so at each iteration one complete field calculation was required (taking approximately 10 seconds on a 1-GHZ Pentium) and 9 derivative calculations, which thanks to the analytic approach took negligible time.

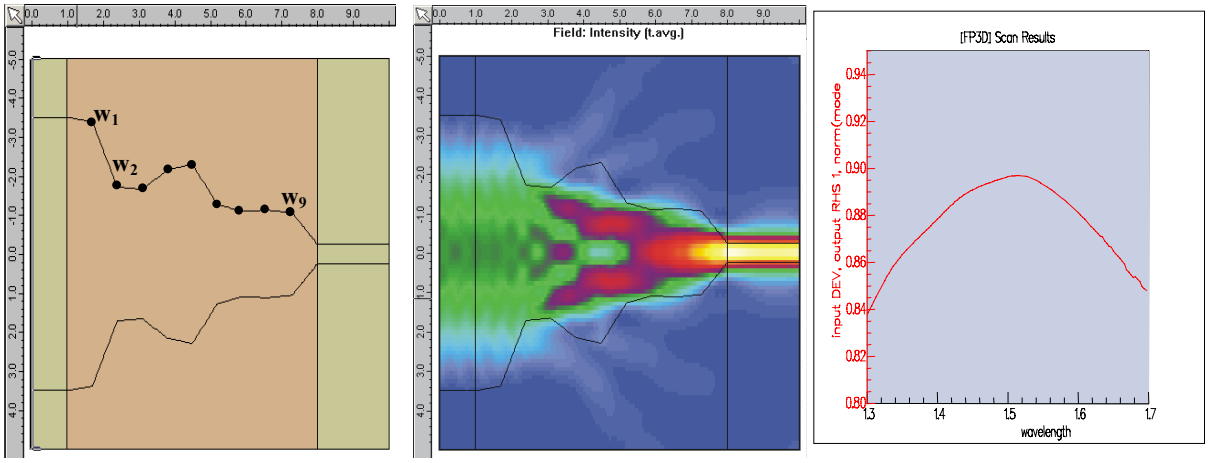

Fig. 3. Optimal shape produced with 9 nodes. Power transmission is now over 90%. The field plot clearly shows the dramatic reduction in radiation loss. The graph on the right is a wavelength scan around the working wavelength.

The interesting field pattern appearing in the optimised structure indicates that this highly optimal transmission is not due to an increased adiabatic effect, but to the exploitation of resonance effects between the local modes. The local modes are defined as being the z-varying coefficients $C_m(z)$ of the eigenmode expansion of the field in terms of the modes $\psi_m(x,y;z)$ at the cross section of the waveguide at a given position z,

$$\Phi(x,y,z) = \sum_{m>=1} \psi_m(x,y;z) \cdot (c_m^+(z).e^{i\beta_m(z)z} + c_m^-(z).e^{-i\beta_m(z)z}) .$$

As seen in fig.4, these interact in such a way that any power initially coupled into higher order local modes, is re-injected into the fundamental mode at the RHS exit.

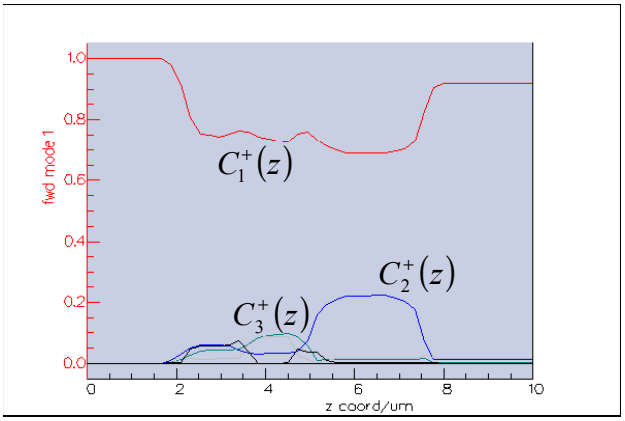

Fig. 4. Excitation in the local modes along the length of the optimised taper. Note how the power which is initially lost from the fundamental mode (red line) is gradually "passed back" into lower modes: eg. From mode mode 3 (green line) into mode 2 (the blue line) and then back into the fundametal mode.

IMPROVING THE WAVELENGTH INSENSITIVITY

The main drawback of these structures seems to be their wavelength sensitivity: in the above example the transmission decreases to 87% when varying by 0.1µm either way. In an attempt to improve this we re-launched the optimization with the objective function given by the sum of power transmission at three different wavelengths: the working wavelength (1.51µm), and 0.4µm either side. Fig. 5 shows the new structure. Not only is the power transmission even better (92%), it also remains virtually unchanged in the wavelength window specified in the objective function.

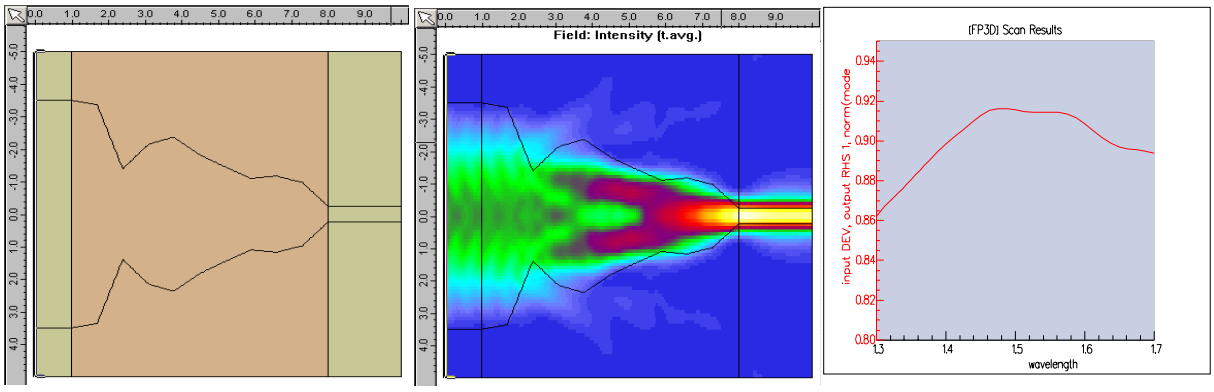

Fig. 5. Result of optimizing over 3 wavelengths. Field plot is for wavelength = 1.51 µm. Not only is the power transmission is even better (92%), it also remains virtually unchanged in the wavelength window 1.47 µm to 1.55 µm.

VARYING THE LENGTH OF THE OPTIMAL TAPER.

In the previous section we found the optimal shape for a given fixed taper length. We now repeat the optimisation for different taper lengths. We find that the optimal shapes will tend to vary considerably, but the field shape in these optimal tapers will always have the same pattern, following the same resonance mechanism described above (fig. 6). Note however how the optimal taper shape becomes more "jagged" as the length is decreased. Clearly, for shorter lengths, larger shape variations are required to achieve the desired optimal resonance effect. The transmission remains near perfect for decreasing lengths, until a certain minimum critical length is reached, below which the optimal resonance effect can no longer exist (fig. 7).

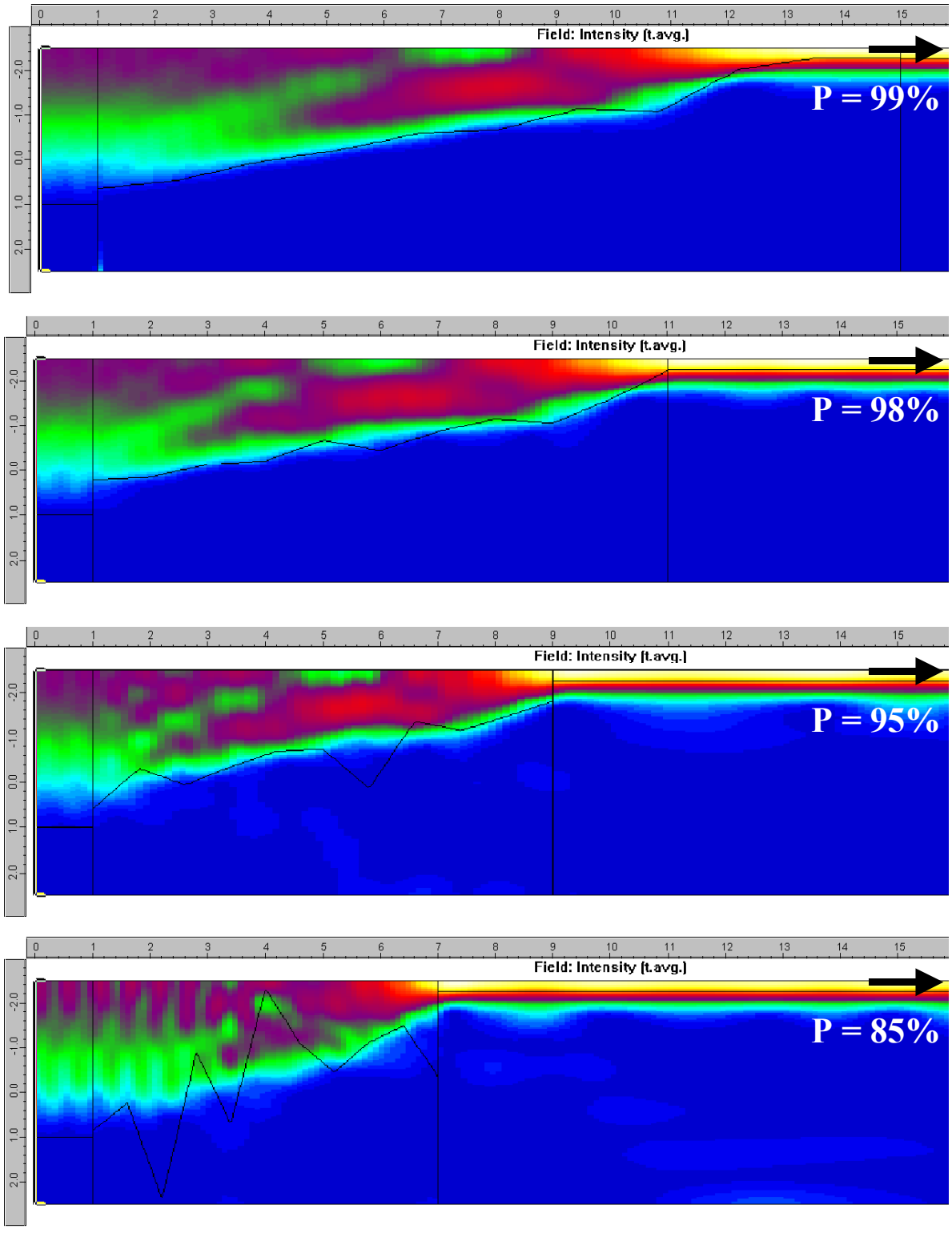

Fig. 6. Optimal shapes at different lengths: 14µm, 10µm, 8µm, 6µm. The optimiser always tended to choose a profile giving the resonant field structure. Note that in these examples we have also allowed the ends to vary freely, thus introducing two extra degrees of freedom. This had the effect of improving the transmission at a given length.

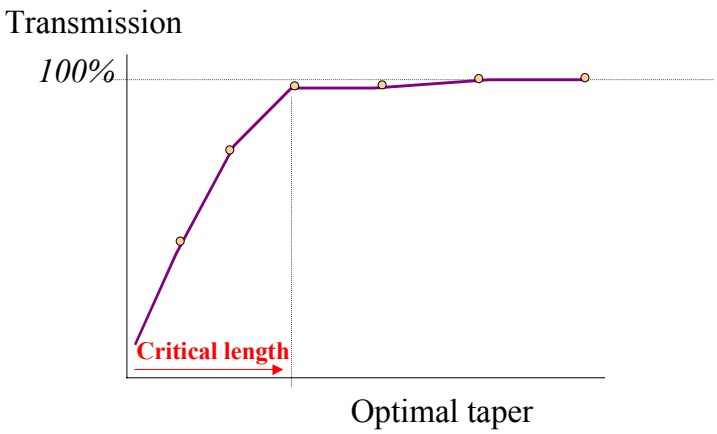

Fig. 7. Transmission vs. length of optimal taper. The transmission is near perfect for all lengths above a certain threshold but then decreases rapidly for smaller lengths.

HIGHER DISCRETISATIONS.

Increasing the number of nodes would be the natural choice in attempting to improve on these results, as it is assumed that the more degrees of freedom in the optimization, the better the optimal solution. This indeed is true but it should be noted that the more the number of variables, the more unstable the optimization process becomes. This makes it easier for the optimizer to fall into local minima corresponding to highly irregular structures, which may have good transmission at the working wavelength, but are highly sensitive to wavelength perturbations. This drawback is solved to some extent by doing a multiple wavelength optimization shown above. However the number of wavelength sampling points in the objective may need to increase with the number of nodes, making the optimization problem more calculation intensive. Optimisation problems of this sort, involving large degrees of freedom are closely linked to inverse scattering problems in electrodynamics, and exhibit similar computational complications. For a detailed discussion on these instability issues, as well as techniques for solving these problems, we refer the reader to [6].

OPTIMISING PHOTONIC CRYSTALS.

We now consider the problem of optimising the power transmission within a hexagonal photonic crystal lattice. 100% transmission within line defects can be achieved using wavelengths within the crystal band gap, however it is still unclear how to design splitters and bends which eliminate back-reflections. In this study we look at how transmission can be maximised in a photonic crystal bend. The optimal design of splitters will be the subject of another paper.

The crystal lattice we consider here has a material with effective cross-sectional index of 2.5. The air holes have diameter 0.35μm and the spacing between them is 0.5μm (fig. 8). The band gap for such a crystal lies between wavelengths 1.32um and 1.54um. We chose 1.4um as the working wavelength.

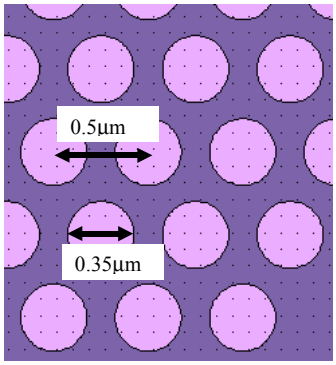

Fig. 8. Photonic Crystal structure: A hexagonal confugutation of air holes in a medium of effective index of 2.5

SETTING UP THE PROPAGATION PROBLEM.

Again, we use mode matching techniques for solving the propagation problem for a given wavelength. As with the taper example, the entire photonic crystal domain is subdivided into thin, z-invariant sections. The problem is reduced to finding both forward and backward modal excitations c_m^+, c_m^- for the field in each of these sections.

Care needs to be taken in setting up the problem, as we wish to measure the transmitted power travelling in a given line-defect (Bloch) mode. This does not correspond to a given modal excitation. We therefore choose to solve the problem of calculating the total power *P* exiting on the right hand side given by the excitation of the fundamental mode of a guide on the LHS (Fig 9). Preliminary numerical experiments show that the power in the fundamental mode carried by the input wavegude is totally transmitted into the fundamental Block mode of the crystal structure, irrespective of the waveguide width, penetration into the crystal, or of the waveguide effective index. This is true providing the waveguide width is smaller that the line defect width, and the effective index contrast with the crystal material is sufficiently low to avoid internal reflections at the waveguide end (but not too low, as it must carry at least one guided mode). In our case an effective index of 2.51 turns out to be an appropriate choice.

The is RHS output designed to eliminate the reflections back into the line-defect, so that the total power exiting the crystal channel is the same as the power exiting the RHS of the computational domain. This can easily be calculates in terms of the modal excitation coefficients o the RHS: $P = \sum_{m>=1} \left| C_m^+ \right|^2$

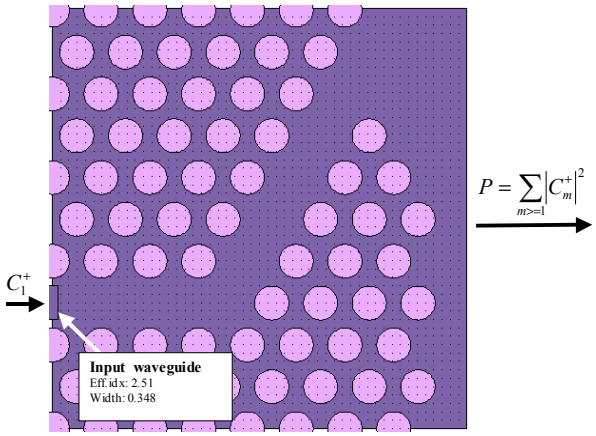

Fig. 9. The line defect bend with the input waveguide on the LHS and the empty region on the RHS. The total transmiterd power is then just the sum of the powers in the forward moving coefficients the input waveguide is engineered to couple its funfamental mode into the fundamental crystal Bloch mode.

SOLVING THE OPTIMIZATION PROBLEMS

We considered the optimisation problem of maximizing the total power transmission P by varying the position and size of various holes around the bend region. As it was quite likely the many sub-optimal configurations may occur, we resorted to using the global optimisation routine contained in KALLISTOS. This technique systematically subdivides the parameter space, using an internal algorithm to split more quickly in regions most likely to contain an optimum. Since the entire parameter space is eventually explored, this optimisation technique is not only guaranteed to (eventually) find the globally optimal solution, but can also show other interesting local optima. This is in contrast to the better known Genetic Algorithms, which use stochastic search criteria to converge on one single optimum, which is likely, but not guaranteed, to be the global one. However The increased robustness of global optimisation techniques comes at a price: they do require many more calculations than a local descent algorithm to achieve comparable accuracy.

SETTING UP AND RUNNING THE OPTIMISATION

We attempt to optimise the transmission by varying a group of atoms: two "satellite" atoms S1, S2 placed along the input and output line defects and a group of six atoms X1,…,X6 placed in a hexagonal shape round the bend origin (fig.10). The variables to be optimised are:

- the distance L of S1, S2 along the line defect,
- their diameter D,
- the hexagon radius R,
- the diameter D1 of X1,…,X6.

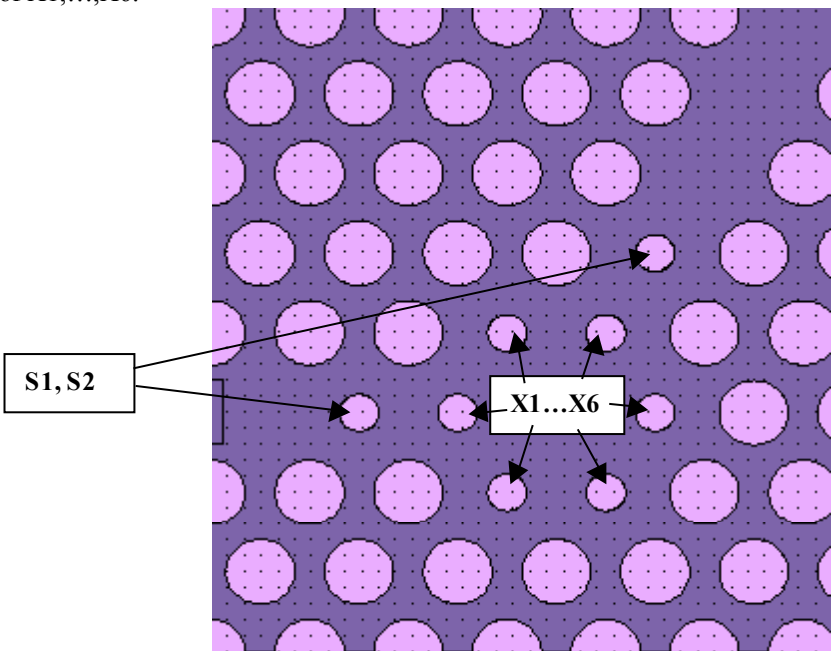

Fig. 10. The variable holes in the line defect.

As each field calculation takes approximately 1 minute on a 1GhZ machine, the program was left to run overnight to calculate 1600 points in the parameter space. The results of the optimiser can be seen in Fig. 11. The optimal solutions appear as accumulation points in the parameter space projections, where the optimiser concentrated its search.

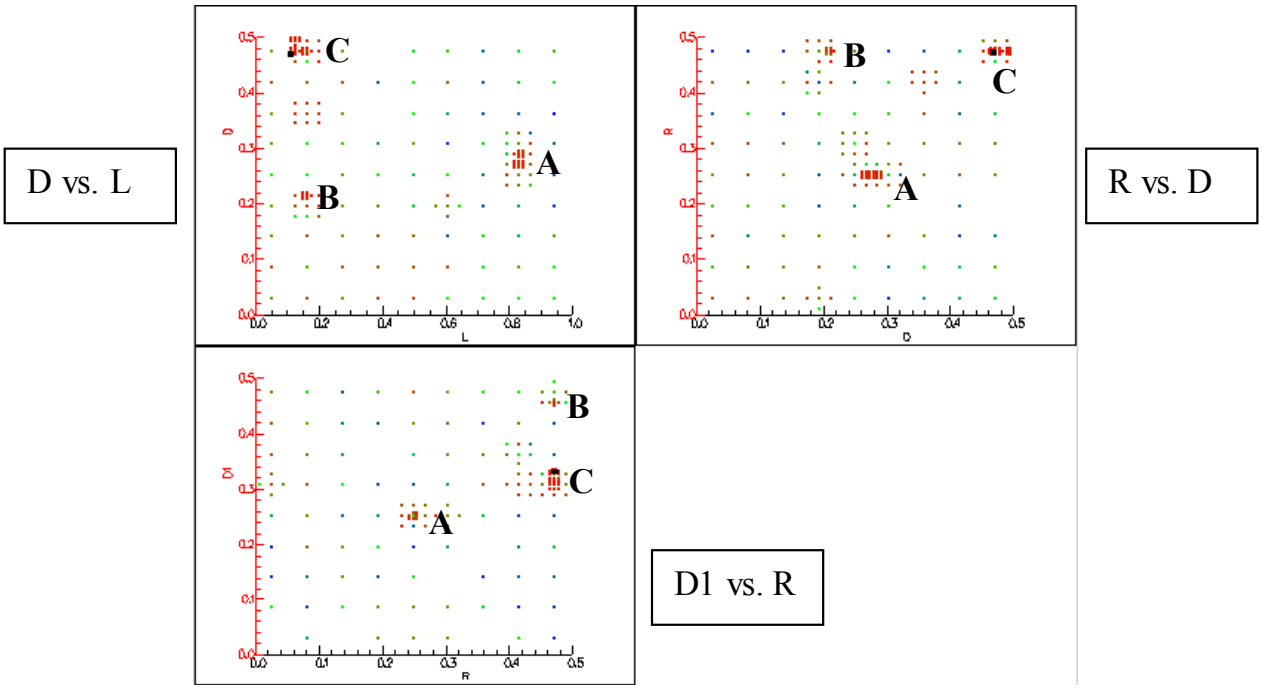

Fig 11. Projections (D vs. L), (R vs. D), (D1 vs. R) in the parameters space (L , R, D , D1) showing the points calculated by the KALLISTOS global optimiser. Three cumulation points A,B,C appear in each graph, corresponding to potentially optimal solutions.

THE OPTIMAL SOLUTIONS

These three points correspond to quantitatively distinct optimal transmission mechanisms. The least efficient of these, labelled "C", achieves improved transmission using a resonant mini ring cavity sorrounding the bend providing a feedback loop (Fig. 12). The next point, "B", has much better transmission, achieved via a small resonance cavity on the outer corner of the bend (Fig. 13). The point with best transmission, "A", has the holes positioned in such a way as to form a "side mirror" on the outer edge of the bend. Note how the hexagonal holes X1,…X6, have been repositioned exactly to match the crystal structure (Fig. 14).

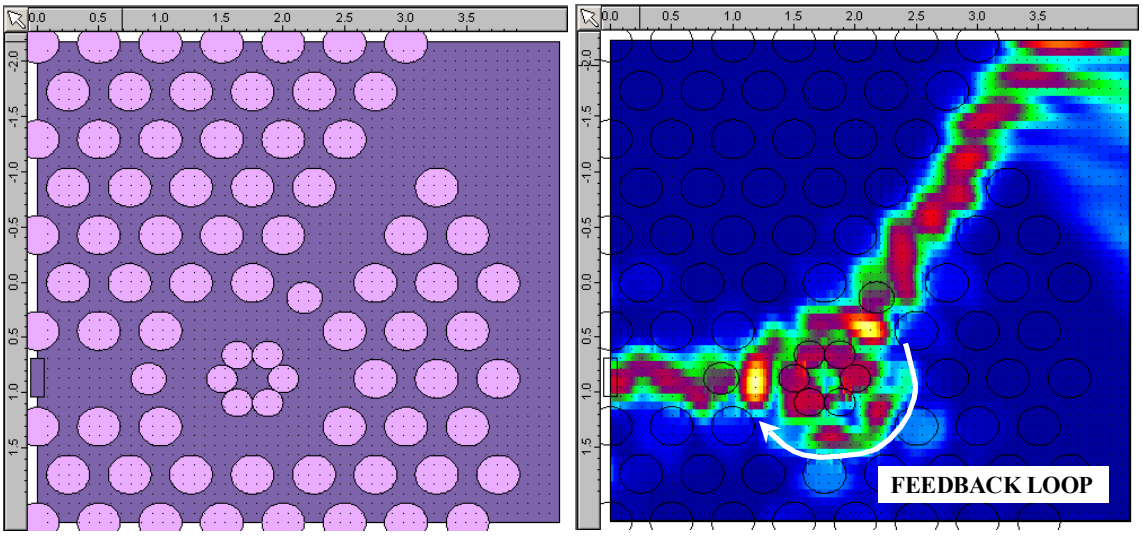

Fig. 12. Optimal configuration A. L=0.84μm , D=0.28μm , R=0.25μm , D1=0.25μm. Transmitted power: 88%. Optimal transmission is achieved using a resonant mini ring cavity sorrounding the bend providing a feedback loop.

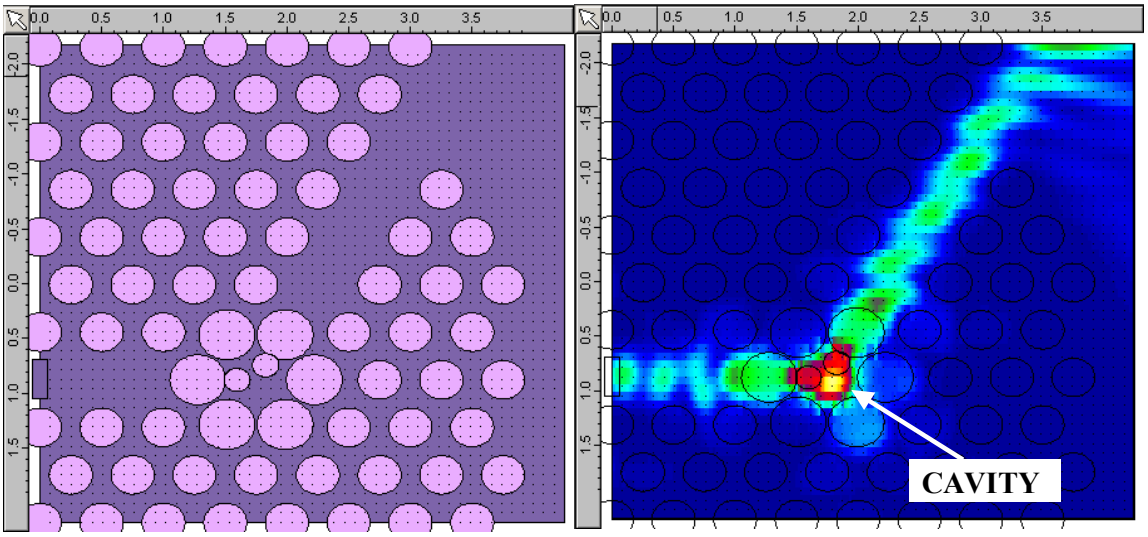

Fig. 13. Optimal configuration B. L=0.15µm , D=0.21µm , R=0.47µm , D1=0.45µm. Transmitted power: 93%. Optimal transmission achieved via a small resonance cavity on the outer corner of the bend.

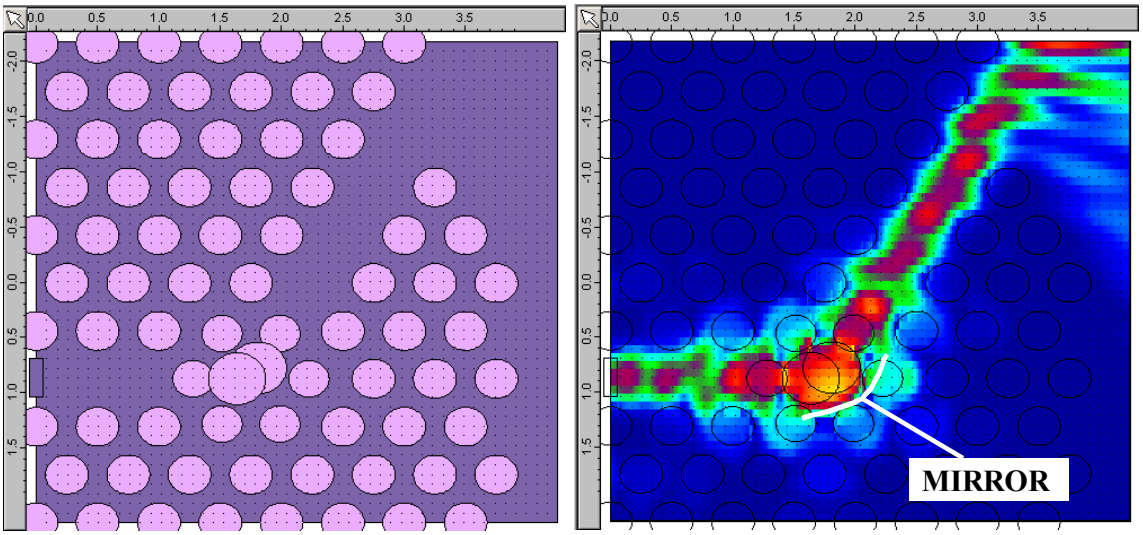

Fig. 14. Optimal configuration C. L=0.11µm , D=0.47µm , R=0.47µm , D1=0.33µm. Transmitted power: 94%. This uses reflections off a mirror formed on the outer side of the bend to optimise the transmission.

This example illustrates how appropriate GLOBAL optimisation techniques can be used not only to find the globally optimum solution in problems containing many local optima, but can also give insights into entirely different, and unexpected, mechanisms for achieving optimal transmissions. These can be used as the starting point for new design ideas further exploiting these new transmission mechanisms to produce even better performances.

CONCLUSION AND OUTLOOK

Using state of the art local optimization techniques combined with an accurate Maxwell solver it is possible to design high contrast, very short injection devices with relatively good wavelength insensitivity. Considerable speed improvements are achieved by exploiting the structure of the wave equations to calculate the descent direction in each iteration step. The applications of such devices are varied, but they could provide the way to integrate injection devices interfacing a fibre or planar waveguide and, say, a photonic-crystal component directly onto the photonic chip. The methods used herein have applicability to many other problems such as design of tapered fiber filters [7], and optimized fiber index profiles.

We have also shown how global optimisation techniques can be used to discover novel configurations in photonic crystal structures giving improved transmissions. The insights gained into their underlying transmission mechanisms provide new ideas in the pursuit of configurations in photonic crystal lattices with optimal performances for bends, splitters, etc.

REFERENCES

1. J. D. Love and W. J. Stewart, W.H. Henry, R. J. Black, S. Lacroix, and F. Gonthier, "Tapered single-mode fibers and devices: I. Adiabaticity criteria", idem, 138 (5) 343-354 (1991).
2. R. J. Black, S. Lacroix, F. Gonthier and J. D. Love, "Tapered single-mode fibers and devices: II. Local-mode power evolution", idem, 138 (5) 355-364 (1991).
3. R. J. Black, F. Gonthier, S. Lacroix, J. Lapierre and J. Bures, "Tapered fibers: an overview", invited paper, Proc. SPIE. 839, 2-19, (1987).
4. R. J. Black, F. Gonthier, A. Hénault and S. Lacroix, "Comparison between Beam Propagation Method and Coupled-Mode simulations for non-uniform guides with circular symmetry", Topical Meeting on Integrated Photonics Research (Optical Society of America) (1990).
5. FIMMPROP propagation tool. Photon Design, 34 Leopold Street, Oxford OX41TW, UK. Email: info@photond.com. Web: http://www.photond.com
6. T. Felici and H.W. Engl, “On shape optimisation of optical waveguides”, Inverse Problems 17, 1141-1162 (2001)
7. F. Gonthier, S. Lacroix, X. Daxhelet, R. J. Black and J. Bures, "Compact all-fiber wavelength filter synthesis for 1300/1550nm demultiplexing isolation", Proc. S.P.I.E. 988, 22-26 (1988).
8. KALLISTOS optimisation tool. Lambdatek, 34 Leopold Street, Oxford OX41TW, UK. Email: info@lambda-tek.com. Web: http://www.lambda-tek.com